

Article

Coupling Coordination Degree of AOD and Air Pollutants in Shandong Province from 2015 to 2020

Ping Wang ¹, Qingxin Tang ^{1,*} , Yuxin Zhu ², Yaqian He ³ , Quanzhou Yu ¹, Tianquan Liang ¹ and Yuying Ran ¹¹ College of Geography and Environment, Liaocheng University, Liaocheng 252059, China² School of Urban and Environmental Sciences, Huaiyin Normal University, Huaian 223300, China³ Department of Geography, University of Central Arkansas, Conway, AR 72034, USA

* Correspondence: tangqingxin@lcu.edu.cn

Abstract: In order to reveal the correlation between aerosols and pollution indicators, the MODIS aerosol optical depth (AOD) was used to investigate the distribution of AOD in 16 prefecture-level cities in Shandong Province from 2015 to 2020. This study quantitatively analyzed the coupling degree and the coupling coordination degree between AOD and pollution indicators based on the coupling coordination model. The results showed that: (1) The annual average AOD in Shandong Province showed a rapid downward trend with a mean value of 0.615. The seasonal AOD of Shandong Province and prefecture-level cities was characterized by spring and summer > autumn and winter. The distribution of AOD in Shandong Province showed a spatial pattern of high in the west and low in the east, and high in the surrounding area and low in the middle. The decreasing rate of AOD was high in the west and low in the east. (2) The annual average AOD and Air Quality Index (AQI) were in a highly coupled and coordinated state. Their spatial distribution pattern decreased from west to east. There were certain fluctuations with seasonal changes, with the largest fluctuation in winter. (3) Except for O₃, the overall coupling and coordination level between AOD and each pollutant was relatively high. The coupling coordination effect was as follows: C (PM_{2.5}, AOD) and C (PM₁₀, AOD) > C (NO₂, AOD) > C (SO₂, AOD), and C (CO, AOD) > C (O₃, AOD). Except for the O₃, its distribution was characterized by highs in the west and lows in the east. The degree of coupling between each pollution indicator and the seasonal average AOD was high. The study showed that there was a high degree of coupling and coordination between pollutant concentration indicators and AOD, and remote sensing AOD data can be used as an effective supplement to regional pollutant monitoring indicators.

Keywords: Shandong Province; AOD; pollutants; coupling coordination degree; MODIS

Citation: Wang, P.; Tang, Q.; Zhu, Y.; He, Y.; Yu, Q.; Liang, T.; Ran, Y. Coupling Coordination Degree of AOD and Air Pollutants in Shandong Province from 2015 to 2020.

Atmosphere **2023**, *14*, 654. <https://doi.org/10.3390/atmos14040654>

Academic Editors: Alessia Sannino, Alejandro Rodríguez-Gómez and Simone Lolli

Received: 23 February 2023

Revised: 27 March 2023

Accepted: 29 March 2023

Published: 30 March 2023



Copyright: © 2023 by the authors. Licensee MDPI, Basel, Switzerland. This article is an open access article distributed under the terms and conditions of the Creative Commons Attribution (CC BY) license (<https://creativecommons.org/licenses/by/4.0/>).

1. Introduction

As an important part of the ecological environment, the atmosphere is closely linked to humans. Aerosols are mixtures of tiny solid and liquid-suspended particles in the atmosphere, with a standard radius of 0.001 to 100 μm [1]. Atmospheric aerosol particles can originate from human activities, such as biomass burning and industrial emissions, or from natural processes, such as wildfires, desert dust, and sea spray [2–4]. The absorption and scattering of radiant energy by atmospheric aerosols can alter atmospheric stability, thereby affecting cloud microphysics, lifetime, and other properties [5]. Aerosols have a strong influence on the earth-atmosphere radiation budget and the global climate [6,7]. Aerosols are blamed for deteriorating visibility and air quality [8]. Air pollution presents a human health risk [9,10] and is associated with mortality [11]. Particulate matter with a diameter less than 2.5 μm , or PM_{2.5}, is able to penetrate deeply into the cardiovascular system and lung, hence presenting a tremendous human health risk [12]. As the main indicator for analyzing the spatial and temporal characteristics of aerosols, the aerosol optical depth (AOD) is an important physical parameter that accurately reflects the atmospheric turbidity [13]

and air quality [14] in a certain range. A better understanding of the spatial and temporal distribution of AOD and its change pattern is important for environmental improvement and sustainable development.

The influence of pollutants cannot be ignored in the assessment of ambient air quality. SO_2 , NO_2 , CO , and O_3 have an important influence on the formation of atmospheric aerosols [15,16], while fine particulate matter ($\text{PM}_{2.5}$) and respirable particulate matter (PM_{10}) are important constituents of near-surface aerosols [17]. Meanwhile, the study of the relationship between AOD and the air quality index (AQI) has attracted many scholars [18]. Many studies have been conducted to investigate the link between AQI, pollutants, and AOD. Tsai et al. [19] assessed the air quality conditions in the region with the help of AOD and $\text{PM}_{2.5}$ data in Taiwan from 2006 to 2008, showing a clear and strong seasonality between the two. Similarly, Li et al. [20] analyzed the AOD- $\text{PM}_{2.5}$ relationship by a Combined Maximum Covariance Analysis (CMCA) to compare all-sky and clear-sky data. The results showed that AOD and $\text{PM}_{2.5}$ were consistent in terms of interannual variability. Meanwhile, there was a good agreement between AOD and $\text{PM}_{2.5}$ in regions of the eastern United States. Srekanth et al. [21] explored the correlation between AOD and $\text{PM}_{2.5}$ mass concentrations over five Indian megacities for four consecutive years using linear and multiple regressions and verified a positive correlation between AOD and $\text{PM}_{2.5}$. In addition to $\text{PM}_{2.5}$, Shi et al. [22] found a good indication of AOD on AQI by exploring the correlation between the Moderate Resolution Imaging Spectroradiometer (MODIS) AOD and AQI in Xiamen based on geographic information system (GIS) technology and statistical regression methods. More comprehensively, Ruan et al. [23] analyzed the correlation between AOD and AQI, $\text{PM}_{2.5}$, PM_{10} , SO_2 , NO_2 , CO , and O_3 in Kunming city in 2018 and found that the correlations between AOD and AQI, $\text{PM}_{2.5}$, PM_{10} , and O_3 concentrations were significantly positive. Identifying the correlation between AOD and pollutants in different regions can improve the estimation of ground-monitored pollutant concentrations [24,25]. It can also provide a scientific basis for environmental quality improvement.

Most of the existing studies have studied the relationship between AOD and air pollutants by constructing linear or curvilinear regression models [26–28]. Yet, there are problems of temporal incongruence and incomplete spatial matching between AOD obtained from remote sensing data and atmospheric pollutants [29]. Therefore, the regression models may lead to the occurrence of temporal and spatial misalignments of AOD and pollutants. These coupling models can effectively address this issue. Coupling is the phenomenon of two or more systems interacting with each other through various interactions; it originated in physics but is now widely used in climate change and environmental studies [30]. The degree of coupling and its coordination determine the order and structure of the system when it reaches the critical region. That is to say, it determines the characteristics and laws of the phase transition of the system in the process from disorder to order [31]. The coupling coordination models can be used to obtain the coupling coordination degree of AOD and AQI and different pollution indicators and to analyze the coupling law in spatial and temporal distribution. This can provide a theoretical reference for air pollution and environmental management.

At present, studies on the relationship between AOD and pollutant indicators using coupled models mostly focus on the period of strong pollution, which fails to reflect its overall nature and change process [32]. Moreover, the research areas of the relevant studies are mostly concentrated in economically developed cities or regions, such as the Beijing-Tianjin-Hebei urban agglomeration [33,34]. Rapid urbanization and industrialization during the past decades have led to a deterioration in the air quality across China [35,36], such as in the North China Plain [37,38]. Heavy anthropogenic pollution caused by industrial and agricultural activities and urbanization has resulted in aerosols with rather complex physical and optical properties [39,40]. In the eastern part of the North China Plain (Figure 1), Shandong province is one of the most polluted and populous regions in China [41]. In 2019, five cities in Shandong were in the bottom 20 in terms of air quality, according to a study of 168 major cities in China [42]. These cities included Zaozhuang, Linyi, Liaocheng, Jinan, and Zibo.

Despite the severe air quality issue in the province, there has been little study to explore the AOD and its associations with different pollutants. Timely monitoring of the changes in AOD and understanding the link between AOD and AQI, pollutant indicators, can play a key role in environmental improvement in Shandong Province. To achieve this aim, this study examined the spatial and temporal distribution characteristics and change patterns of AOD from 2015 to 2020 based on MOD04_3K AOD products in Shandong Province. We selected PM_{2.5}, PM₁₀, SO₂, NO₂, CO, and O₃ as pollution indicators and combined them with a coupled coordination model to obtain the coupling coordination degree of AOD with different pollution indicators and AQI to reveal its coupling mechanism in the spatial and temporal distribution of Shandong Province.

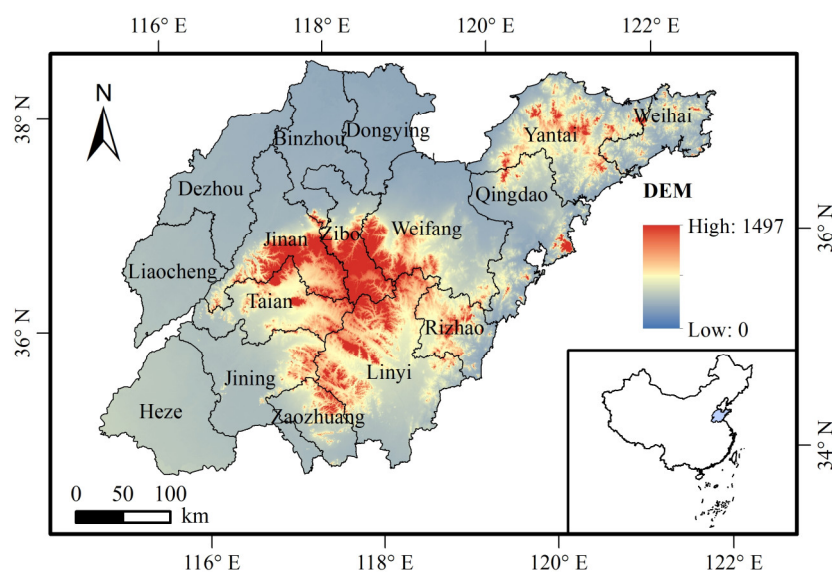


Figure 1. Study area.

2. Data and Methods

2.1. Data

As one of the main sensors carried on Terra and Aqua satellites, the moderate resolution imaging spectroradiometer (MODIS) is a widely used aerosol detection sensor with a high update frequency and wide spectral range [43]. This study selected the Level 2 MOD04_3K AOD product released by NASA from 2015 to 2020. This product is a new 3 km daily aerosol product based on the Dark Target (DT) aerosol algorithm for obtaining the optical properties (e.g., optical depth and size distribution) and mass concentrations of atmospheric aerosols in the global marine and terrestrial environments [44,45]. Many studies have been conducted to validate the product within China and have found that the MODIS 3 km aerosol product quality is stable, the overall inversion accuracy is high, and the data results are reliable [46–48].

Daily averages of AQI and air pollutant concentration data (including PM_{2.5}, PM₁₀, SO₂, NO₂, CO, and O₃) for 16 prefecture-level cities in Shandong Province from 2015 to 2020 were obtained from Sky Cloud (<https://www.ebd120.com>, accessed on 2 July 2021), a site whose data originated from the China General Environmental Monitoring Station and the real-time ambient air quality release platforms of provinces and cities.

2.2. Methods

2.2.1. Linear Regression Trend Analysis

In this study, a unary linear regression model ($y = kx + b$) is used to analyze the trend of AOD in prefecture-level cities from 2015 to 2020. The X-axis is the year (time series), the Y-axis is the AOD, and the slope k represents the tendency rate. When $k > 0$, the

result indicates that the AOD exhibits a trend of growth, and vice versa. The formula for calculating the k is as follows:

$$k = \left(n \sum_{i=1}^n i X_i - \sum_{i=1}^n i \sum_{i=1}^n X_i \right) / \left[n \sum_{i=1}^n i^2 - \left(\sum_{i=1}^n i \right)^2 \right] \quad (1)$$

where n is the number of years (i.e., 6 in this study); i is the i th year (i.e., 2015 is the first year); and X_i is the annual average value of the AOD in the i th year.

2.2.2. Standardization of Pollution Indicators

Since the units of measurement are different among pollution indicators, it is necessary to standardize the indicators, that is, to convert the absolute values of the indicators into relative values. This study used extreme value standardization, which is shown in Equation (2). Since indicator data may be 0 after the extreme value normalization, a positive number slightly greater than 0 should be added to the result of such data. In this study, 0.001 is added to avoid the meaninglessness of the assigned number [49], as shown in Equation (3).

$$X_j = \frac{X_i - X_{min}}{X_{max} - X_{min}} \quad (2)$$

$$X_j = \frac{X_i - X_{min}}{X_{max} - X_{min}} + 0.001 \quad (3)$$

In Equations (2) and (3), X_j denotes the j th data of the standardized index, X_i denotes the i th data of the original pollutant index, X_{min} denotes the minimum value in the original pollutant index data, and X_{max} denotes the maximum value in the original pollutant index data.

2.2.3. Coupling Degree Model

The degree of coupling is used to describe the degree of interaction between two or more systems or system elements [50]. Borrowing from the concept of capacity coupling in physics, the following model is obtained:

$$U = 2 \sqrt{\frac{U_1 U_2}{(U_1 + U_2)^2}} \quad (4)$$

where U denotes the coupling degree of the two system elements, which ranges from 0 to 1; U_1 and U_2 denote the combined indices of the two system elements, i.e., the AOD data as well as the air pollution index data in this study, respectively. The closer U is to 1, the more significant the coupling level is.

2.2.4. Coupling Coordination Degree Model

Both system elements are at low values and may reach a high level of coupling, so we established a coupling coordination degree model [51]:

$$Y = \alpha U_1 + \beta U_2 \quad (5)$$

$$C = (U \times Y)^{\frac{1}{2}} \quad (6)$$

In Equations (5) and (6), C denotes the coupling coordination degree; U denotes the coupling degree; Y denotes the integrated coordination coefficient between aerosols and each air pollution index; α and β denote the contribution coefficients between aerosols and each air pollution index, respectively. In this study, AOD is considered to be equally important as each air pollution index, so α and β are taken as 0.5 [52,53]. The coupling level and coupling coordination level are determined based on coupling degree and coupling coordination degree, respectively, as shown in Table 1.

Table 1. Levels of coupling degree and coupling coordination degree.

U	Coupling Level	C	Coupling Coordination Level
(0.8, 1]	Excellent	(0.8, 1]	Excellent
(0.6, 0.8]	Good	(0.6, 0.8]	Good
(0.5, 0.6]	Normal	(0.5, 0.6]	Normal
(0.4, 0.5]	Less poor	(0.4, 0.5]	Less poor
(0.3, 0.4]	Bad	(0.3, 0.4]	Bad
(0, 0.3]	Worse	(0, 0.3]	Worse

3. Results

This study centers on the AOD, air pollution indicators, and the coupling coordination degree between them for different years and seasons in each prefecture-level city of Shandong Province. To facilitate the study of the characteristics of temporal variation in different quarters, the seasonal variation in the paper is divided into spring from March to May, summer from June to August, autumn from September to November, and winter from December to February [54].

3.1. Spatial and Temporal Variations of AOD

3.1.1. Interannual Variations of AOD

As shown in Figure 2a, the average value of AOD is as high as 0.615 in Shandong Province in the past six years. The annual average AOD value decreases by 0.181 (from 0.724 to 0.543), with an overall decrease of 25%, showing a rapid decreasing trend from 2015 to 2020. The AOD values are different among prefecture-level cities in Shandong Province (Figure 2b and Table 2). The highest average AOD is in Dongying city, with a value of 0.791, while the lowest average AOD is in Yantai city, with a value of 0.460. In the past six years, the AOD values of all prefecture-level cities have decreased, indicating a significant improvement in the atmospheric environment. Among them, the most obvious improvement in AOD is in Tai’an City, with a decline of 32.13%, while Weihai City has the least improvement in AOD, with a decline of 14.98%. In terms of the rate of decrease, the city with the fastest decrease is Dongying, with a value of 0.054, and the slowest is Weihai, with a value of 0.017.

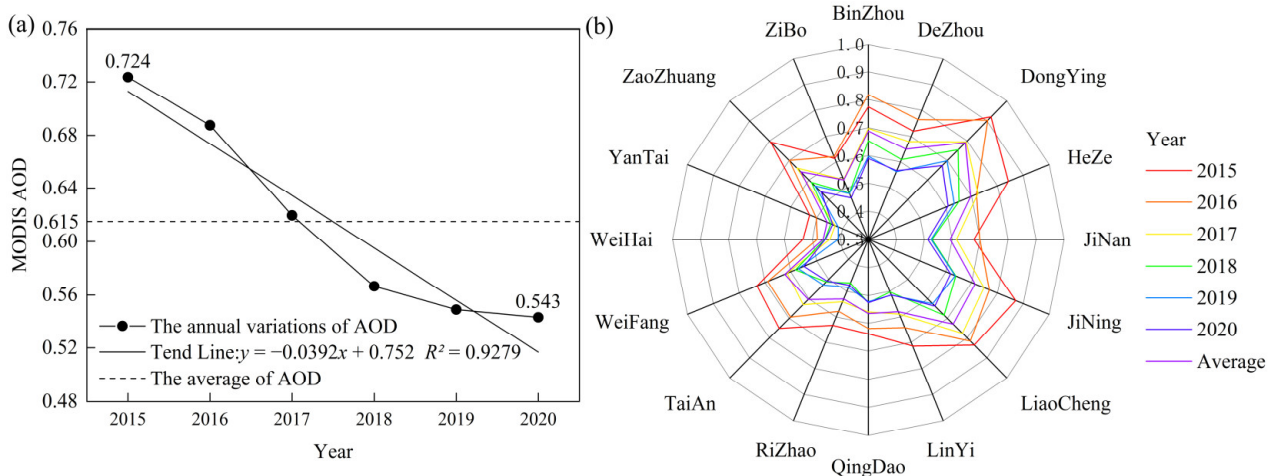


Figure 2. Variations of AOD in (a) Shandong Province and (b) prefecture-level cities from 2015 to 2020.

Table 2. Interannual variations of AOD by prefecture-level cities in Shandong Province from 2015 to 2020.

City	2015	2016	2017	2018	2019	2020	Average	Magnitude of Decrease	k
BinZhou	0.774	0.818	0.698	0.654	0.597	0.590	0.689	23.77%	−0.047
DeZhou	0.720	0.764	0.680	0.610	0.562	0.566	0.650	21.39%	−0.041
DongYing	0.920	0.904	0.795	0.754	0.698	0.674	0.791	26.74%	−0.054
HeZe	0.842	0.719	0.724	0.651	0.632	0.609	0.696	27.67%	−0.043
JiNan	0.677	0.698	0.615	0.528	0.524	0.512	0.592	24.37%	−0.041
JiNing	0.871	0.769	0.748	0.638	0.636	0.618	0.713	29.05%	−0.051
LiaoCheng	0.836	0.816	0.776	0.683	0.625	0.637	0.729	23.80%	−0.048
LinYi	0.714	0.642	0.589	0.503	0.515	0.514	0.580	28.01%	−0.042
QingDao	0.638	0.619	0.559	0.526	0.522	0.526	0.565	17.56%	−0.025
RiZhao	0.633	0.578	0.541	0.467	0.485	0.476	0.530	24.80%	−0.033
TaiAn	0.750	0.693	0.629	0.513	0.528	0.509	0.604	32.13%	−0.052
WeiFang	0.731	0.689	0.614	0.582	0.571	0.550	0.623	24.76%	−0.037
WeiHai	0.534	0.482	0.438	0.455	0.407	0.454	0.462	14.98%	−0.017
YanTai	0.527	0.501	0.429	0.445	0.417	0.438	0.460	16.89%	−0.020
ZaoZhuang	0.794	0.700	0.661	0.588	0.569	0.539	0.642	32.12%	−0.050
ZiBo	0.614	0.621	0.531	0.478	0.476	0.459	0.530	25.24%	−0.036

The spatial distribution of atmospheric aerosols is significantly influenced by topographic features. As shown in Figures 1 and 3a, the distribution characteristics of AOD and elevation in Shandong Province are similar. The distribution of AOD in Shandong Province shows a pattern of being higher in the west, where elevation is relatively low. In the high-elevation regions, the AOD shows low values. Similarly, the decreasing rate of AOD shows a pattern of distribution with high levels in the west and low levels in the east (Figure 3b). The spatial distribution characteristics of AOD found by Lin et al. [55] are similar to this. The fastest-decreasing AOD values are mainly in the western inland cities. Among them, the deceleration of AOD in Dongying city, Tai’an city, and Jining city is above 0.05.

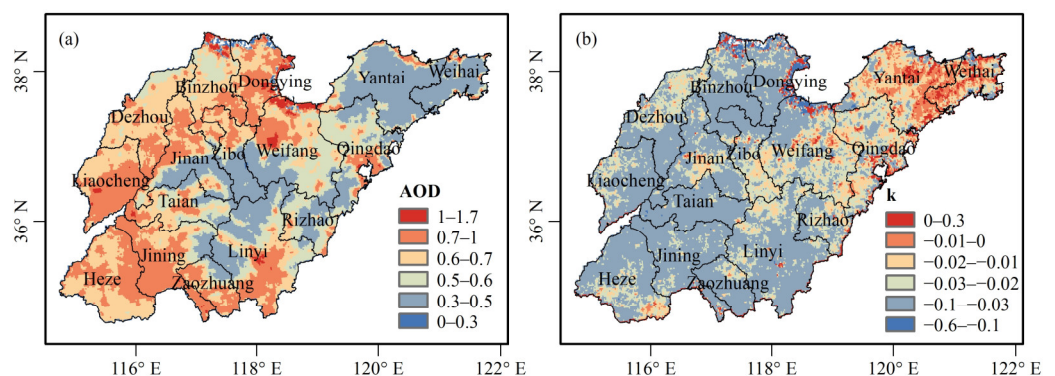


Figure 3. (a) Spatial distribution and (b) decreasing rate of AOD by prefecture level cities in Shandong Province from 2015 to 2020.

3.1.2. Quarterly Variations of AOD

The quarterly average AOD values of Shandong Province for each prefecture-level city from 2015 to 2020 show the characteristics of spring and summer > autumn and winter (Figure 4). Specifically, the quarterly AOD values for most cities are characterized as summer > spring > autumn > winter. The study by Xue et al. [56] on the seasonal distribution of AOD in Shandong Province also showed consistent results. Exceptionally, AOD values in spring are slightly higher in Heze and Zaozhuang than those in summer. There are also differences between AOD values in the prefecture-level cities during the same quarter. The summer AOD values are significantly highest in Dongying city, while

Yantai city and Weihai city have relatively lowest AOD values, which is consistent with the performance of the annual average AOD values in each city (Table 2). The range of fluctuation in AOD values is the largest in the summer.

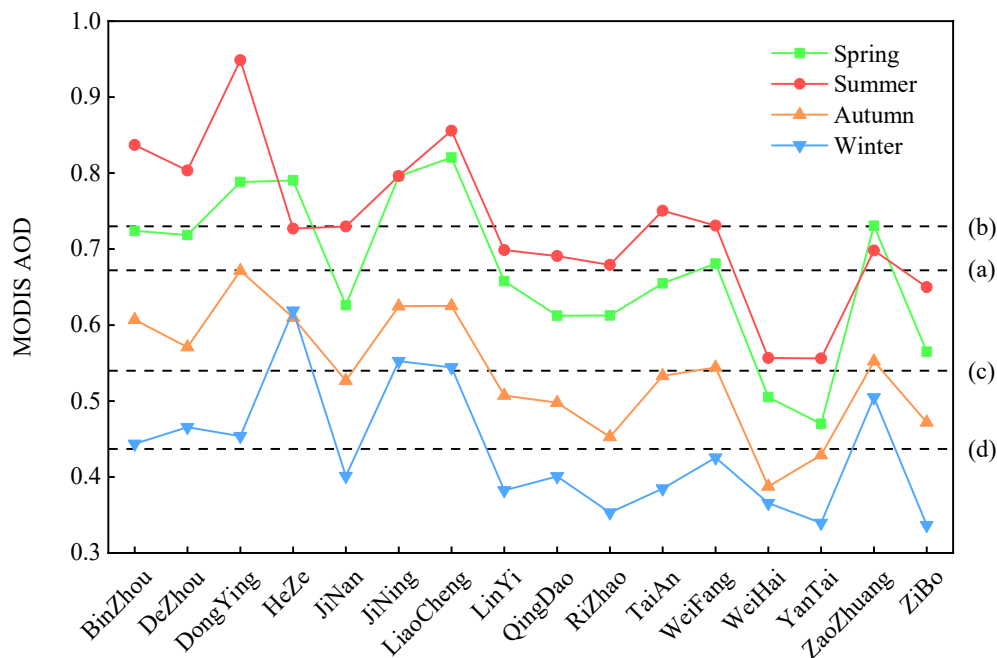


Figure 4. Variations of quarterly AOD by prefecture level cities in Shandong Province: AOD values of Shandong Province in (a) spring, (b) summer, (c) autumn and (d) winter.

3.2. Coupling Degree and Coupling Coordination Degree between AOD and AQI

3.2.1. Interannual Coupling Degree and Coupling Coordination Degree between AOD and AQI

In order to explore the interrelationship between AOD and AQI in each prefecture-level city of Shandong Province, the coupling degree and coupling coordination degree between AOD and AQI were calculated (Table 3). The coupling degree of 13 prefecture-level cities exceeds 0.9. Three-fourths of the prefecture-level cities have coupling coordination above 0.6. However, the coupling degree and coupling coordination between AOD and AQI are lowest in Yantai city.

Table 3. Statistics of coupling degree and coupling coordination degree between AOD and AQI.

City	U	Coupling Level	C	Coupling Coordination Level
BinZhou	0.9992	Excellent	0.8492	Excellent
DeZhou	0.9657	Excellent	0.8660	Excellent
DongYing	0.9847	Excellent	0.9163	Excellent
HeZe	0.9870	Excellent	0.9163	Excellent
JiNan	0.9245	Excellent	0.7728	Good
JiNing	0.9999	Excellent	0.8693	Excellent
LiaoCheng	0.9947	Excellent	0.9500	Excellent
LinYi	0.9310	Excellent	0.7300	Good
QingDao	0.9924	Excellent	0.5303	Normal
RiZhao	0.9403	Excellent	0.5504	Normal
TaiAn	0.9691	Excellent	0.7490	Good
WeiFang	0.9805	Excellent	0.7761	Good
WeiHai	0.6599	Good	0.0515	Worse
YanTai	0.1573	Worse	0.1124	Worse
ZaoZhuang	0.9720	Excellent	0.8366	Excellent
ZiBo	0.7957	Good	0.6548	Good

Figure 5a provides the spatial distribution of the coupling coordination degree between the average AOD and AQI from 2015 to 2020. The coupling coordination degree is higher in six cities in the western part of Shandong Province, while the lowest coupling coordination degree is found in Weihai and Yantai. The coupling coordination degree in Shandong Province clearly shows a decreasing trend from west to east. In addition, there is also some similarity with the distribution of elevation and AOD. Considering that the emissions of 2020 pollutants will be largely affected by the outbreak of the Corona Virus Disease 2019 (COVID-19) in early 2020 [57,58]. We compared the coupling coordination degree between AOD and AQI in 2015, 2019, and 2020 (Figure 5b–d). From 2015 to 2019, the coupling coordination degree between AOD and AQI generally increased, mainly in Binzhou City and Yantai City. However, compared with 2019, the coupling coordination degree between AOD and AQI decreases in 2020, mainly in the cities of Weifang, Zaozhuang, Zibo, and Yantai.

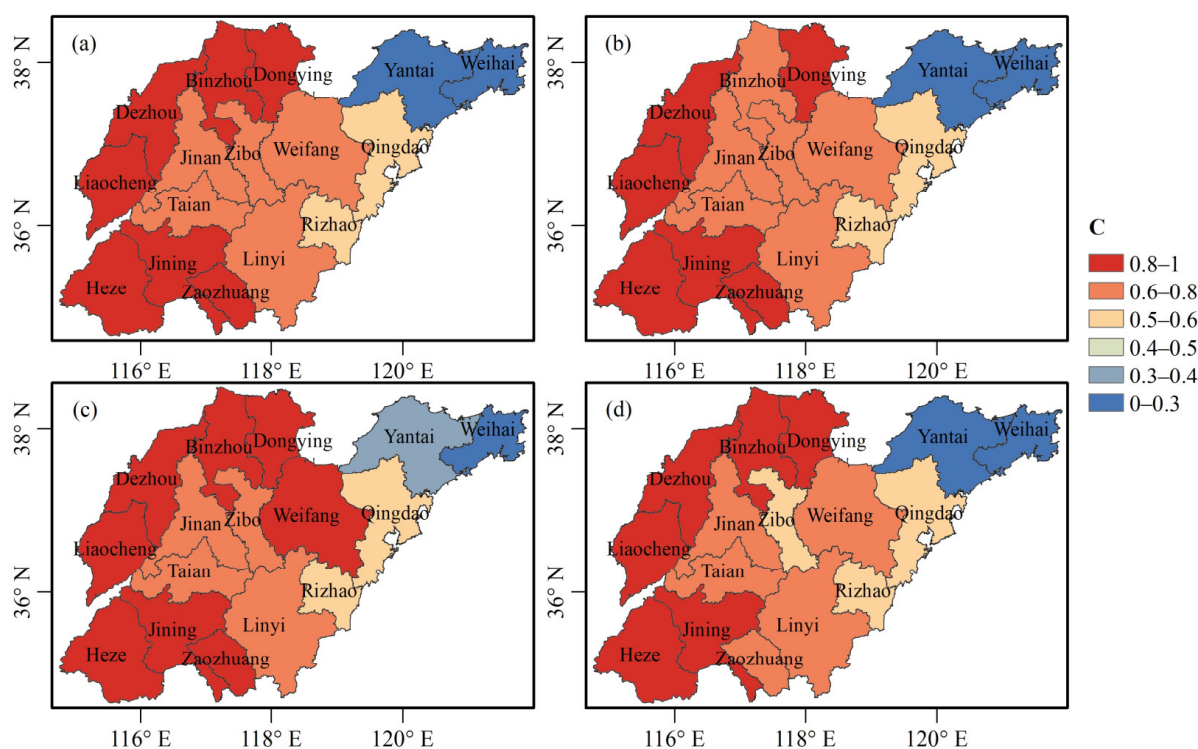


Figure 5. Distribution of coupling coordination degree of Annual average AOD and AQI in prefecture level cities in Shandong Province in (a) 2015~2020, (b) 2015, (c) 2019 and (d) 2020.

3.2.2. Quarterly Coupling Degree and Coupling Coordination Degree between AOD and AQI

The coupling coordination degree of both Weihai city and Yantai city is low in each season, while the coupling coordination degree of Liaocheng city is high (Figure 6). Compared to winter, the coupling coordination degree of the other three seasons for each city fluctuates less and is basically in the same range. Among them, Qingdao city has the smallest fluctuation change in the quarterly coupling coordination level, while Zibo city has the largest fluctuation change.

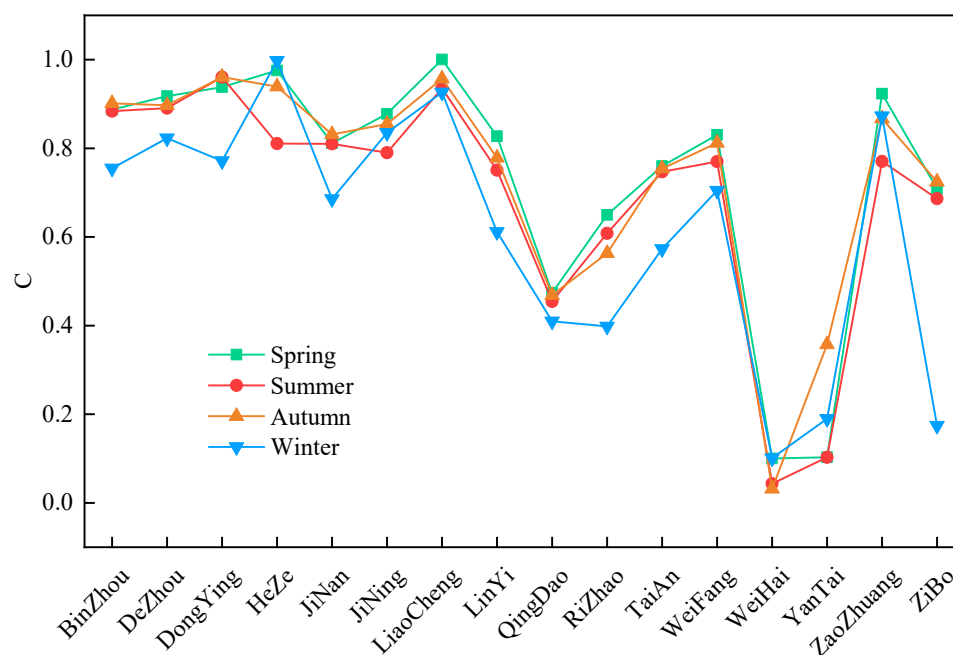


Figure 6. Seasonal change of coupling coordination degree of cities in Shandong Province.

3.3. Coupling Degree and Coupling Coordination Degree between AOD and Pollutants

3.3.1. Interannual Coupling Degree and Coupling Coordination Degree between AOD and Pollutants

The overall trend of the coupling degree between each pollutant indicator and AOD is consistent with the coupling coordination degree (Figure 7). Except for the O_3 , the coupling degree and coupling coordination degree between each pollutant indicator and the AOD are relatively similar, showing a high coupling coordination level in most cities. From the perspective of each pollutant indicator, the coupling coordination effect between $PM_{2.5}$, PM_{10} , and AOD is the most significant. However, there are some differences; for example, the coupling degree of $PM_{2.5}$, PM_{10} , and AOD in Qingdao city is high, but the coupling coordination degree is relatively low. Comparing the four types of gaseous pollutants, the coupling coordination level of AOD with NO_2 is better coordinated. AOD and O_3 also show some coupling coordination phenomena, but they are less obvious compared with other gaseous pollutants. In summary, the coupling coordination level of each pollutant indicator with the annual average AOD from 2015 to 2020 is shown as $C(PM_{2.5}, AOD)$, $C(PM_{10}, AOD)$, $> C(NO_2, AOD)$, $> C(SO_2, AOD)$, and $C(CO, AOD)$, $> C(O_3, AOD)$.

Figure 8 shows that, except for O_3 , the coupling coordination degree between each pollutant indicator and AOD has the characteristics of being high in the west and low in the east. In terms of the level of coupling and coordination between pollutant indicators and AOD, $PM_{2.5}$ and PM_{10} are the highest. In terms of the gaseous pollutant indicators, the coupling coordination degree between NO_2 and AOD is higher. To reflect the changes in the distribution of coupling coordination degree, the distributions of 2015, 2019, and 2020 were also selected for comparison. It is found that except for O_3 , the coupling coordination degrees all show an increase and then a decrease from 2015 to 2020. The areas of change are mainly concentrated in the central region, which is mainly reflected in two types of solid particulate matter, $PM_{2.5}$ and PM_{10} . The coupling coordination degrees between the other three gaseous pollutants and AOD are similar in terms of spatial and temporal variations, except for the large fluctuations of the coupling coordination degrees between O_3 and AOD.

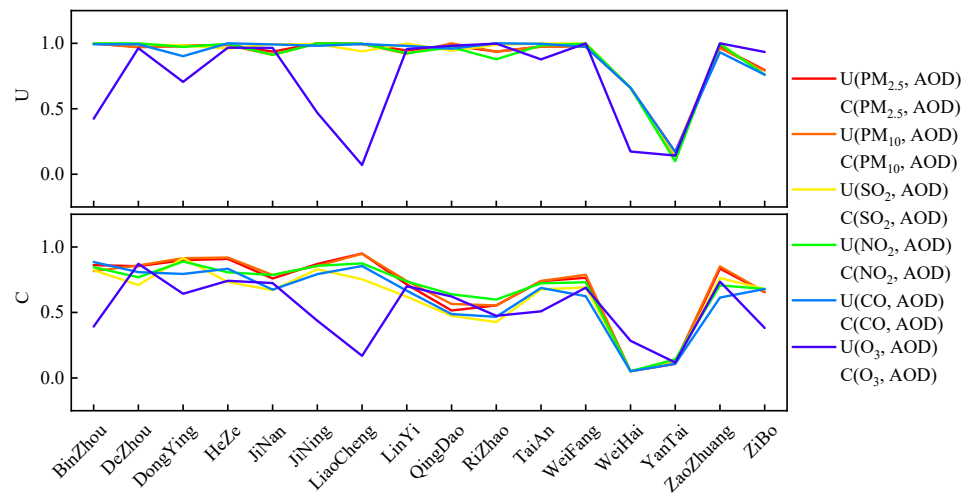


Figure 7. Coupling degree and coupling coordination degree of AOD and each pollution indicator.

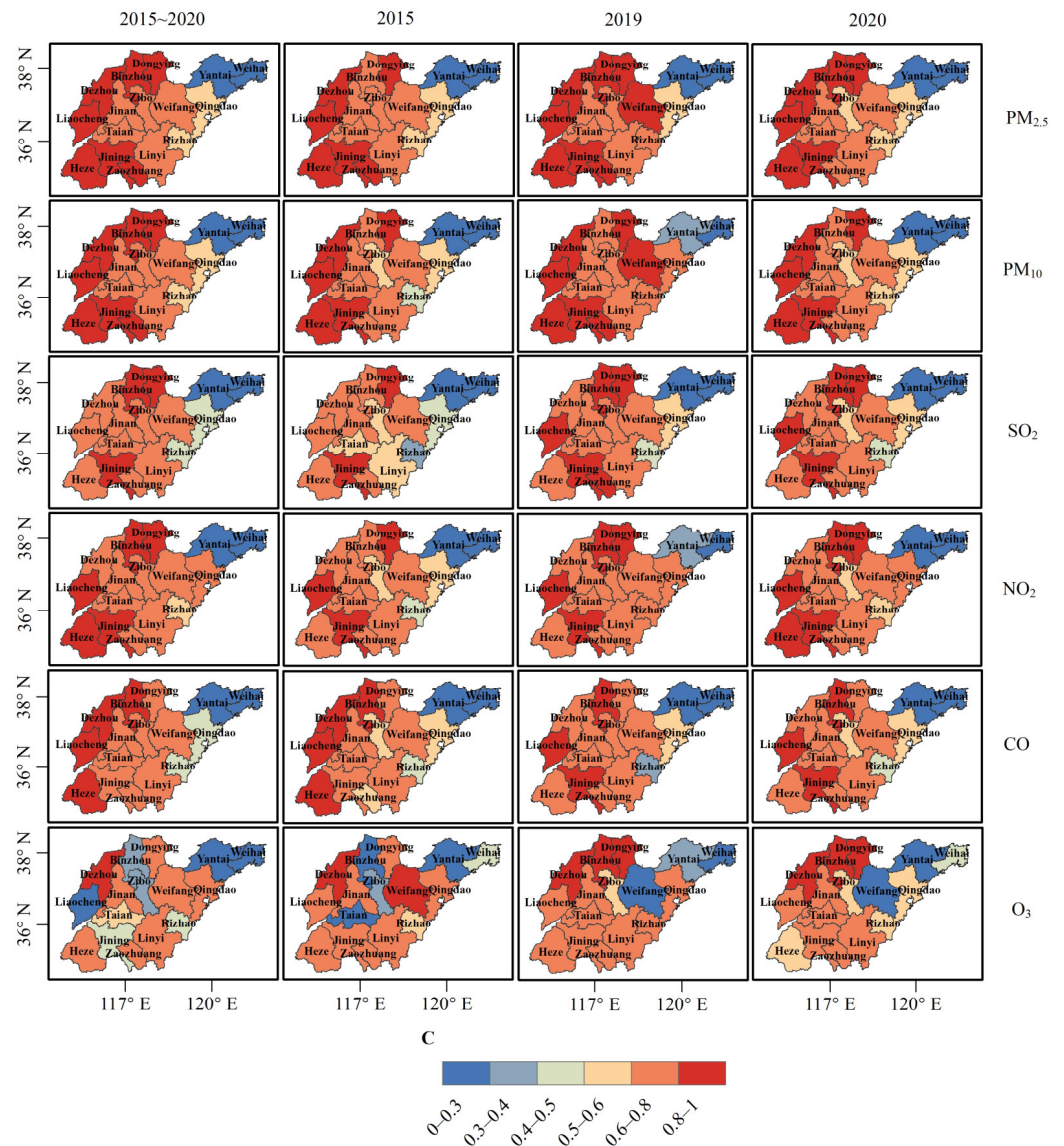


Figure 8. Distribution of coupling coordination degree between Annual average AOD and each pollution indicator in prefecture level cities in Shandong Province in 2015–2020, 2015, 2019, and 2020.

3.3.2. Quarterly Coupling Degree and Coupling Coordination Degree between AOD and Pollutants

The coupling degree between O₃ and AOD fluctuates widely (Figure 9). Yet, the coupling degree between other pollution indicators and AOD is similar in all seasons, showing a high level, although some cities show temporal fluctuations. For instance, the coupling degree in Weihai city and Yantai city is higher in the autumn and lower in the other three seasons. The coupling degree between each pollutant indicator and AOD in Zibo City is greatly lower in winter. In addition, the coupling degree between PM_{2.5} and AOD in Qingdao city is tremendously lower in the summer.

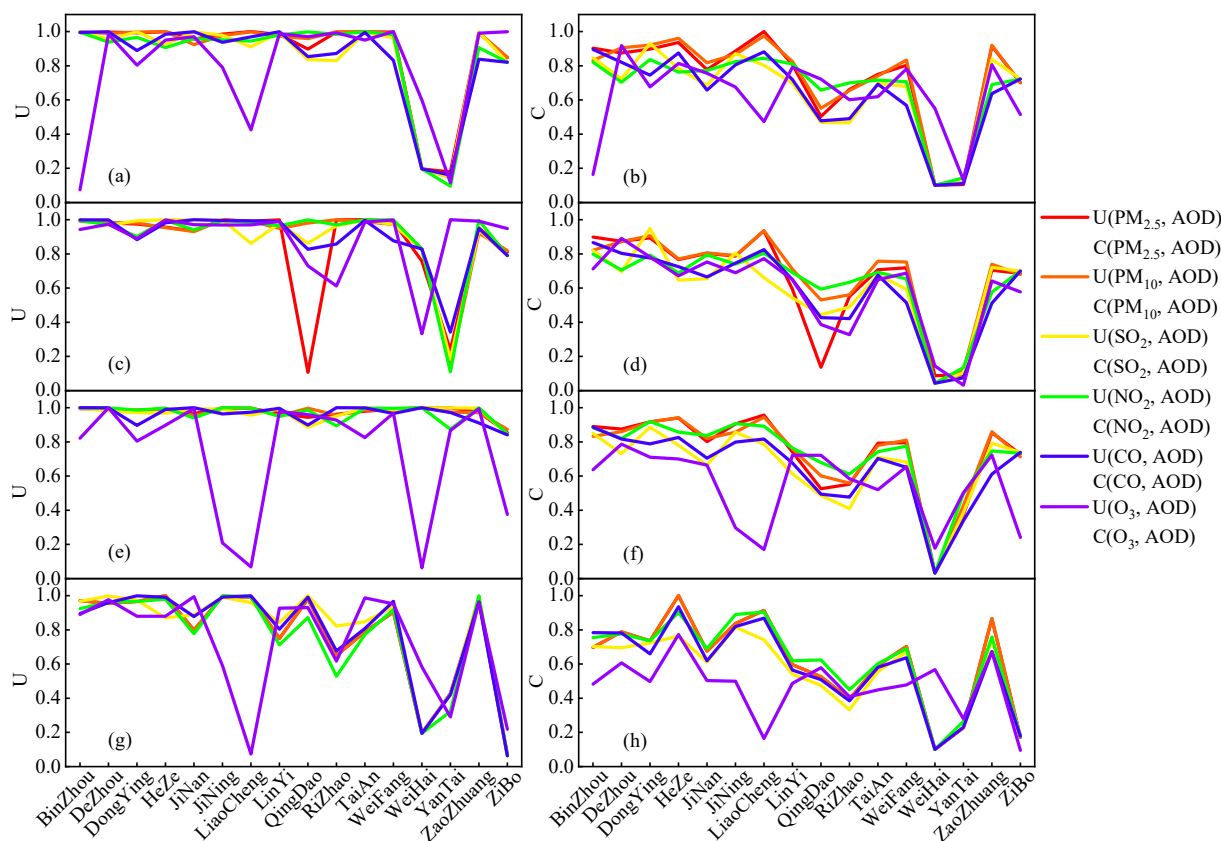


Figure 9. Coupling degree and coupling coordination degree between AOD and each pollution indicator in spring (a,b), summer (c,d), autumn (e,f) and winter (g,h).

The degree of coupling and coordination between the six pollutants and AOD varies among the four seasons and cities. The coupling coordination degree is greater in spring, summer, and autumn than it is in winter. During the four seasons in each prefecture-level city, the coupling coordination degree has the strongest fluctuation amplitude in the winter, while the other seasons have lighter fluctuations. In terms of different pollution indicators, the level of coupling and coordination between O₃ and AOD is remarkably poorer. Except for O₃, the coupling coordination between solid particulate matter and AOD is higher than that of gaseous pollutants.

4. Discussion

4.1. Spatial and Temporal Variations of AOD

According to Figures 2 and 3, it is found that the distribution of AOD in Shandong Province shows a pattern of high in the west and low in the east, high in the surrounding area and low in the middle, influenced by factors such as topography, industrial structure, anthropogenic activities, and the location of sea and land [59]. Similarly, the reduction rate of AOD in Shandong Province shows a characteristic distribution of fast in the west

and slow in the east. In particular, since the 13th Five-Year Plan, the problem of volatile organic compounds (VOCs) in Dongying city has become increasingly prominent [60], and the average AOD value is notably higher. In recent years, the air quality in Dongying city has improved significantly after the application of the government's energy saving and emission reduction policies [61]. Therefore, Dongying city has experienced a significant decrease in AOD values, making it the prefecture-level city with the fastest rate of decrease in Shandong Province over the past six-year period. At the same time, the AOD values for both Tai'an and Jining decline at a rate above 0.05, mainly because of the larger AOD base values. In addition, Yantai and Weihai are typical light industrial cities with little industrial pollution [62]. The air quality is stable and good due to the blocking effect of mountainous terrain [63] and the clean air from the ocean [64]. This makes Yantai and Weihai cities have the lowest AOD values, reduction magnitudes, and decrease rates.

The quarterly average AOD values of Shandong Province from 2015 to 2020 show the characteristics of spring and summer > autumn and winter. In addition to anthropogenic factors, the aerosol hygroscopic effect is pronounced due to high temperatures and high relative humidity in summer [65]. This promotes the increase of AOD values. Whereas, the growth of aerosol particle hygroscopic growth is inhibited in winter due to lower relative humidity. Coupled with short sunshine hours, there are fewer secondary aerosols, resulting in low AOD values in winter [66]. Therefore, the quarterly AOD values of most prefecture-level cities show the characteristics of summer > spring > autumn > winter. This is consistent with the findings of Xue et al. [56] and Nam et al. [67]. However, the spring AOD values in Heze city and Zaozhuang city are slightly higher than those in summer, which may be related to the strong polluted weather and unfavorable diffusion conditions that occurred in spring in recent years [68]. AOD values are higher in the summer and are strongly influenced by inter-regional climate and anthropogenic activities. Therefore, the differences in summer AOD values among prefecture-level cities are large. Among the four seasons, the summer AOD value of Dongying city shows the highest among the prefecture-level cities. Dongying city is located in the Bohai Sea region. Due to the influence of the monsoon, the coastal humidity is high in summer, resulting in the growth of aerosol hygroscopicity [56]. Yantai city and Weihai city have low year-round AOD values, and similarly low AOD values in summer. Furthermore, the differences in AOD values among prefecture-level cities in winter are small. Heze city has the highest AOD value in winter, mainly due to the coal smoke pollution in the main urban area for heating [69].

4.2. Coupling Degree and Coupling Coordination Degree between AOD and AQI

The coupling levels between AOD and AQI from 2015 to 2020 are considered strong. The overall coupling between AOD and AQI is at an excellent level. This indicates that there is a strong interaction between AOD and AQI in Shandong province. Most cities are at excellent and good coupling coordination levels between AOD and AQI. This indicates that the benign coupling levels between AOD and AQI are high. Among them, Yantai City is an anomaly. AQI is strongly influenced by altitude and humidity due to its geographical location [70]. At the same time, the two are affected by natural factors such as meteorology, and the degree and manner of influence are different [18,71,72], resulting in AOD and AQI being in an uncoupled disorder state.

Due to the effects of geographical location, human activities, and other factors, the spatiotemporal heterogeneity of the coupling coordination degree index is relatively obvious (Figure 5a). As shown by the distribution of the coupling coordination between the average AOD and AQI from 2015 to 2020, the six prefecture-level cities in the northwest and southwest regions are clearly at an excellent level of coordination. Since the industrial structure is mostly industrial, the area is strongly influenced by industrial pollution and other human activities. In contrast, Weihai City and Yantai City have worse levels of coupling coordination.

The coupling coordination level between AOD and AQI in 2015, 2019, and 2020 is compared in Figure 5b–d. From 2015 to 2019, the level of coupling coordination between

AOD and AQI in Binzhou and Yantai cities has increased. The benign coupling between AOD and AQI increases, and the relationship gradually tends to be balanced. The coupling coordination level between AOD and AQI decreases in several cities from 2019 to 2020, indicating that their benign coupling decreases. In addition to anthropogenic activities, aerosols and air quality in Shandong Province are influenced by sea breeze, climate, and so on [73,74]. The prevention and control measures of COVID-19 had great restrictions on the movement of people, transportation, engineering construction, industrial production, and commercial trade activities. Industrial emissions and automobile exhaust were greatly reduced, and air quality was significantly improved [75,76]. At the same time, AOD has decreased but still has aerosols from numerous other sources [77]. This makes the benign interaction between AOD and AQI enhance followed by a weakening. In particular, Yantai and Weifang cities show obvious opposite changes before and after the epidemic. The coupling coordination of AOD and AQI both show a change characteristic of rising and then falling. This indicates that anthropogenic activities in Yantai and Weifang have a significant impact on air quality.

Among the same prefecture-level cities, the coupling coordination degree of AOD and AQI shows some fluctuations across the four seasons. The coupling coordination level between AOD and AQI is the lowest in winter, due to the poorer atmospheric quality in Shandong Province in winter [78]. Zibo City is at a worse coordination level in the winter, with a large gap compared to the good levels in the other three seasons. Influenced by the meteorological conditions, it is clearly evident that AOD in winter is the lowest among the four seasons. However, extreme weather in winter often causes poorer air quality [79,80]. Therefore, the coordination between AOD and AQI is poor in the winter.

4.3. Coupling Degree and Coupling Coordination Degree between AOD and Pollutants

By analyzing the coupling level between each pollutant indicator and AOD, we find that AOD has a close coupling relationship with all the pollutants except O_3 . This may be due to a significant negative correlation between aerosols and O_3 [81]. Due to the influence of altitude [82] and location near the ocean [83], Weihai and Yantai cities have low pollution [84] and low aerosol content, resulting in the worst coupling level in relative terms. The overall trend of the coupling coordination between each pollutant indicator and AOD is similar to the coupling level. However, there are exceptions. For example, the degree of interaction between $PM_{2.5}$, PM_{10} , and AOD in Qingdao city is strong, while their coupling coordination levels do not reflect a positive mutual promotion effect. Figure 7 shows that the benign coupling and coordination effect between AOD and solid particulate matter is significantly higher than that between AOD and gaseous pollutants. A similar pattern of results was obtained in the study of the coupling coordination between AOD and pollutants in the Beijing-Tianjin-Hebei region by Hao et al. [52]. Specifically, the coupling and coordination level of each pollutant indicator with AOD from 2015 to 2020 shows $C(PM_{2.5}, AOD), C(PM_{10}, AOD) > C(NO_2, AOD) > C(SO_2, AOD),$ and $C(CO, AOD) > C(O_3, AOD)$.

Except for O_3 , the coupling coordination between each pollutant indicator and AOD has a distribution characteristic of high in the west and low in the east, similar to the spatial distribution of AOD (Figure 8). This may be influenced by anthropogenic activities and geographical location [85]. Weihai and Yantai cities are obviously influenced by the small concentrations of pollutants and AOD. Their coordination effects are always poorly constrained. By comparing the distribution changes of the coupling coordination degree in 2015, 2019, and 2020, it is found that the change in the coordination relationship between gaseous pollutants and AOD is great for solid particulate matter. In addition, the cities with changes are mostly located in the central part of Shandong Province. However, in general, the changes in coordination levels show a trend of increasing and then decreasing from 2015 to 2020, except for O_3 . This indicates that the benign interaction between the pollutants and AOD is first enhanced and then weakened. It is more obvious that the changes in coordination levels of AOD and PM_{10} , SO_2 , NO_2 , and CO in Zibo City are all

from normal to good and then to normal. Pollutant concentrations were significantly lower due to the strong influence of the COVID-19 pandemic [86,87]. This caused a consistent downward trend in their coupled coordination.

There is a close coupling between each pollutant and AOD in all seasons, except for O_3 . Exceptionally, the interaction between $PM_{2.5}$ and AOD is remarkably weak in Qingdao city in summer. This is mainly due to the high rainfall in summer, which reduces the particulate matter content in the atmosphere [88]. The degree of coupling and coordination between different pollutants and AOD is different in the four seasons. Pollutant levels are significantly higher in the winter [89], while AOD is lower relative to other seasons, influenced by climatic factors. There is a clear difference in tendency between the two elements, resulting in poor coordination in winter. Except for O_3 , the coupling coordination degree between solid particulate matter and AOD is significantly higher than that of gaseous pollutants. This is consistent with the pattern of coupling coordination between AQI and AOD.

5. Conclusions

During the period of 2015 to 2020, the average value of AOD in Shandong Province was as high as 0.615. The annual average AOD decreased by 25% with a rapid downward trend, indicating a significant improvement in the atmospheric environment. Similar to the characteristics of the altitude in Shandong Province, the distribution of AOD in Shandong Province showed a pattern of high in the west and low in the east, high in the surrounding area, and low in the middle. Similarly, the decreasing rate of AOD also showed a pattern of high concentration in the west and low concentration in the east. Influenced by anthropogenic activities and climatic factors, the quarterly average AOD values of Shandong Province and prefecture-level cities from 2015 to 2020 showed that spring and summer > autumn and winter. Specifically, the quarterly AOD values of most cities showed the characteristics of summer > spring > autumn > winter. The mean AOD values varied widely between cities in the same quarter, with the largest differences in summer.

From 2015 to 2020, the coupling level between AOD and AQI in Shandong province was considered strong. The coupling coordination between AOD and AQI clearly showed a spatial distribution trend of decreasing from west to east and a temporal change trend of increasing and then decreasing. On a quarterly scale, the coupling coordination between AOD and AQI fluctuated somewhat with the seasons, with the greatest fluctuation in winter. The high coupling coordination between AOD and AQI provided a theoretical basis for using remote sensing AOD data as an effective supplementary means for AQI monitoring at the regional scale. This can compensate to a certain extent for the shortcoming of the insufficient spatial density of AQI ground observation sites.

The overall trend of the coupling coordination degree between each pollutant indicator and AOD was similar to the coupling degree. There was a close coupling relationship between AOD and all pollutants except O_3 . Specifically, the degree of coupling coordination between each pollutant indicator and AOD in 2015–2020 was shown as $C(PM_{2.5}, AOD)$, $C(PM_{10}, AOD)$, $> C(NO_2, AOD)$, $> C(SO_2, AOD)$, and $C(CO, AOD) > C(O_3, AOD)$. Except for O_3 , the coupling coordination of each pollutant index with AOD had the characteristic of being high in the west and low in the east. The coupling coordination phenomenon was significant in areas with low altitude and high population density or industrial activities. The changes in the coupling coordination degree of each pollutant index and AOD all showed a trend of increasing first and then decreasing. The changes were mainly concentrated in the central part of Shandong Province and were mainly reflected in two types of solid particles, $PM_{2.5}$ and PM_{10} . In addition, the degree of coupling coordination among prefectures fluctuated the most in the winter. However, the coupling coordination degree in winter was significantly lower than that in the other three seasons.

Furthermore, O_3 and AOD showed different degrees of coupling coordination and changes in different areas. Therefore, comprehensive pollution control measures should be implemented in a targeted manner based on further pollution traceability analysis. Due to

the limitations of available data, the pollutant data selected for this study are ground-based observations. AOD is the integration of the extinction coefficient of a medium in the vertical direction, which is often related to the vertical distribution of pollutants. However, there is also unevenness in the vertical distribution of pollutants. Therefore, how the unevenness in the vertical direction affects the correlation between AOD and pollutants will be the next research direction.

Author Contributions: Conceptualization, Q.T.; methodology, P.W. and Q.T.; software, P.W. and Q.T.; validation, Q.T.; formal analysis, P.W.; investigation, P.W. and Q.T.; resources, P.W.; data curation, P.W. and Q.T.; writing—original draft preparation, P.W.; writing—review and editing, P.W., Q.T., Y.Z., Y.H., Q.Y., T.L. and Y.R.; visualization, P.W.; supervision, Q.T.; project administration, Q.T.; funding acquisition, Q.T., T.L. and Q.Y. All authors have read and agreed to the published version of the manuscript.

Funding: This research was funded by the National Natural Science Foundation of China, grant numbers 31800367 and 41971025, and the Natural Foundation of Shandong Province of China, grant numbers ZR2021MD090 and ZR2017MD017.

Institutional Review Board Statement: Not applicable.

Informed Consent Statement: Not applicable.

Data Availability Statement: The datasets analyzed during the current study mainly include the MOD04_3K AOD product and the AQI and air pollutant concentration data. The MOD04_3K AOD product is available in the National Aeronautics and Space Administration (NASA) Goddard Space Flight Center (<https://earthdata.nasa.gov/>, accessed on 6 May 2022). The AQI and air pollutant concentration data are available in SkyCloud (<https://www.ebd120.com>, accessed on 2 July 2021).

Acknowledgments: We would like to thank the NASA Earth Data website (<https://earthdata.nasa.gov/>, accessed on 6 May 2022) for providing MODIS aerosol and auxiliary products.

Conflicts of Interest: The authors declare no conflict of interest.

References

1. Ali, M.A.; Bilal, M.; Wang, Y.; Qiu, Z.; Nichol, J.E.; de Leeuw, G.; Ke, S.; Mhawish, A.; Almazroui, M.; Mazhar, U.; et al. Evaluation and comparison of CMIP6 models and MERRA-2 reanalysis AOD against Satellite observations from 2000 to 2014 over China. *Geosci. Front.* **2022**, *13*, 101325. [[CrossRef](#)]
2. Tao, M.; Wang, J.; Li, R.; Wang, L.; Wang, L.; Wang, Z.; Tao, J.; Che, H.; Chen, L. Performance of MODIS high-resolution MAIAC aerosol algorithm in China: Characterization and limitation. *Atmos. Environ.* **2019**, *213*, 159–169. [[CrossRef](#)]
3. Tariq, S.; Qayyum, F.; Ul-Haq, Z.; Mehmood, U. Long-term spatiotemporal trends in aerosol optical depth and its relationship with enhanced vegetation index and meteorological parameters over South Asia. *Environ. Sci. Pollut. Res.* **2022**, *29*, 30638–30655. [[CrossRef](#)] [[PubMed](#)]
4. ul-Haq, Z.; Tariq, S.; Ali, M. Spatiotemporal patterns of correlation between atmospheric nitrogen dioxide and aerosols over South Asia. *Meteorol. Atmos. Phys.* **2017**, *129*, 507–527. [[CrossRef](#)]
5. Ali, G.; Bao, Y.; Ullah, W.; Ullah, S.; Guan, Q.; Liu, X.; Li, L.; Lei, Y.; Li, G.; Ma, J. Spatiotemporal Trends of Aerosols over Urban Regions in Pakistan and Their Possible Links to Meteorological Parameters. *Atmosphere* **2020**, *11*, 306. [[CrossRef](#)]
6. Mishra, A.K.; Koren, I.; Rudich, Y. Effect of aerosol vertical distribution on aerosol-radiation interaction: A theoretical prospect. *Heliyon* **2015**, *1*, e00036. [[CrossRef](#)]
7. Samset, B.H.; Stjern, C.W.; Andrews, E.; Kahn, R.A.; Myhre, G.; Schulz, M.; Schuster, G.L. Aerosol Absorption: Progress Towards Global and Regional Constraints. *Curr. Clim. Chang. Rep.* **2018**, *4*, 65–83. [[CrossRef](#)]
8. Ching, J.; Kajino, M. Aerosol mixing state matters for particles deposition in human respiratory system. *Sci. Rep.* **2018**, *8*, 8864. [[CrossRef](#)]
9. Shindell, D.; Kuylensstierna, J.C.I.; Vignati, E.; van Dingenen, R.; Amann, M.; Klimont, Z.; Anenberg, S.C.; Muller, N.; Janssens-Maenhout, G.; Raes, F.; et al. Simultaneously Mitigating Near-Term Climate Change and Improving Human Health and Food Security. *Science* **2012**, *335*, 183–189. [[CrossRef](#)]
10. Wang, Z.; Liu, Y.; Hu, M.; Pan, X.; Shi, J.; Chen, F.; He, K.; Koutrakis, P.; Christiani, D.C. Acute health impacts of airborne particles estimated from satellite remote sensing. *Environ. Int.* **2013**, *51*, 150–159. [[CrossRef](#)]
11. Dockery, D.W.; Pope, C.A.; Xu, X.; Spengler, J.D.; Ware, J.H.; Fay, M.E.; Ferris, B.G.; Speizer, F.E. An Association between Air Pollution and Mortality in Six U.S. Cities. *N. Engl. J. Med.* **1993**, *329*, 1753–1759. [[CrossRef](#)]
12. Pope, C.A.; Dockery, D.W. Health Effects of Fine Particulate Air Pollution: Lines that Connect. *J. Air Waste Manag. Assoc.* **2006**, *56*, 709–742. [[CrossRef](#)] [[PubMed](#)]

13. Khoshshima, M.; Bidokhti, A.A.; Ahmadi-Givi, F. Variations of aerosol optical depth and Angstrom parameters at a suburban location in Iran during 2009–2010. *J. Earth Syst. Sci.* **2014**, *123*, 187–199. [[CrossRef](#)]
14. Alföldy, B.; Osán, J.; Tóth, Z.; Török, S.; Harbusch, A.; Jahn, C.; Emeis, S.; Schäfer, K. Aerosol optical depth, aerosol composition and air pollution during summer and winter conditions in Budapest. *Sci. Total Environ.* **2007**, *383*, 141–163. [[CrossRef](#)]
15. Wu, J.; Zhang, Y.; Wang, T.; Qian, Y. Rapid improvement in air quality due to aerosol-pollution control during 2012–2018: An evidence observed in Kunshan in the Yangtze River Delta, China. *Atmos. Pollut. Res.* **2020**, *11*, 693–701. [[CrossRef](#)]
16. Quan, J.; Wang, Q.; Ma, P.; Dou, Y.; Liao, Z.; Pan, Y.; Cheng, Z.; Ding, D.; Jia, X. Secondary aerosol formation in cloud serves as a vital source of aerosol in the troposphere. *Atmos. Environ.* **2021**, *253*, 118374. [[CrossRef](#)]
17. Sun, Y.; Du, W.; Wang, Q.; Zhang, Q.; Chen, C.; Chen, Y.; Chen, Z.; Fu, P.; Wang, Z.; Gao, Z.; et al. Real-Time Characterization of Aerosol Particle Composition above the Urban Canopy in Beijing: Insights into the Interactions between the Atmospheric Boundary Layer and Aerosol Chemistry. *Environ. Sci. Technol.* **2015**, *49*, 11340–11347. [[CrossRef](#)]
18. Chen, Y.; Li, D.; Karimian, H.; Wang, S.; Fang, S. The relationship between air quality and MODIS aerosol optical depth in major cities of the Yangtze River Delta. *Chemosphere* **2022**, *308*, 136301. [[CrossRef](#)] [[PubMed](#)]
19. Tsai, T.-C.; Jeng, Y.-J.; Chu, D.A.; Chen, J.-P.; Chang, S.-C. Analysis of the relationship between MODIS aerosol optical depth and particulate matter from 2006 to 2008. *Atmos. Environ.* **2011**, *45*, 4777–4788. [[CrossRef](#)]
20. Li, J.; Carlson, B.E.; Laci, A.A. How well do satellite AOD observations represent the spatial and temporal variability of PM2.5 concentration for the United States? *Atmos. Environ.* **2015**, *102*, 260–273. [[CrossRef](#)]
21. Sreekanth, V.; Mahesh, B.; Niranjana, K. Satellite remote sensing of fine particulate air pollutants over Indian mega cities. *Adv. Space Res.* **2017**, *60*, 2268–2276. [[CrossRef](#)]
22. Shi, Y.; Deng, Q.; Wu, J.; Wang, J. Regression analysis of MODIS aerosol optical thickness and air quality index in Xiamen City. *Remote Sens. Land Resour.* **2020**, *32*, 106–114. [[CrossRef](#)]
23. Ruan, O.; Liu, S.; Chen, F.; Chen, Y.; Luo, J.; Liang, P.; Yu, M. Correlation analysis between modis AOD and air pollutant concentration in Kunming city. *J. Guizhou Norm. Univ. Nat. Sci.* **2021**, *39*, 21–29. [[CrossRef](#)]
24. Sorek-Hamer, M.; Franklin, M.; Chau, K.; Garay, M.; Kalashnikova, O. Spatiotemporal Characteristics of the Association between AOD and PM over the California Central Valley. *Remote Sens.* **2020**, *12*, 685. [[CrossRef](#)]
25. Kamarul Zaman, N.A.F.; Kanniah, K.D.; Kaskaoutis, D.G. Estimating Particulate Matter using satellite based aerosol optical depth and meteorological variables in Malaysia. *Atmos. Res.* **2017**, *193*, 142–162. [[CrossRef](#)]
26. Zeng, W.; Hao, Q.; Zhao, Z.; Xiong, W.; Chen, J.; Xin, J.; Jiang, C. Characteristics of Aerosol Optical Depth in the Urban Area of Beibei and Its Correlation with Particle Concentration. *Environ. Sci.* **2020**, *41*, 1067–1077. [[CrossRef](#)]
27. Shao, P.; Xin, J.; An, J.; Kong, L.; Wang, B.; Wang, J.; Wang, Y.; Wu, D. The empirical relationship between PM2.5 and AOD in Nanjing of the Yangtze River Delta. *Atmos. Pollut. Res.* **2017**, *8*, 233–243. [[CrossRef](#)]
28. Xiao, Z.; Xie, X.; Lin, X.; Xie, J.; Chen, J.; Shi, Y.; Chen, Y. The spatio-temporal characteristics of aerosol optical thickness as well as the relationship with PM2.5 in Xiamen city, China. *Environ. Monit. Assess.* **2020**, *192*, 676. [[CrossRef](#)]
29. Zhang, J.; Zhao, Y.; Tian, Y.; He, Q.; Zhang, Y.; Peng, Y.; Hong, S. Spatial non-coupling of air pollutant emissions and particulate matter-related air quality: A case study in Wuhan City, China. *Prog. Geogr.* **2019**, *38*, 612–624. [[CrossRef](#)]
30. Li, Y.; Li, Y.; Zhou, Y.; Shi, Y.; Zhu, X. Investigation of a coupling model of coordination between urbanization and the environment. *J. Environ. Manag.* **2012**, *98*, 127–133. [[CrossRef](#)]
31. Liu, Q.; Wang, L. Examination of a coupling coordination relationship between urbanization and the eco-environment: Case study of Hangzhou. *Acta Sci. Circumstantiae* **2018**, *38*, 4214–4222. [[CrossRef](#)]
32. Sun, L.; Wang, A.; Wang, J. Spatial Characteristics Analysis for Coupling Strength among Air Pollutants during a Severe Haze Period in Zhengzhou, China. *Int. J. Environ. Res. Public Health* **2022**, *19*, 8224. [[CrossRef](#)] [[PubMed](#)]
33. Yao, L.; Xu, Y.; Sun, S.; Wang, Y. Revisiting PM2.5 pollution along urban-rural gradient and its coupling with urbanization process, a new perspective from urban pollution island analysis. *Urban Clim.* **2022**, *45*, 101270. [[CrossRef](#)]
34. Li, X.; Lu, Z.; Hou, Y.; Zhao, G.; Zhang, L. The coupling coordination degree between urbanization and air environment in the Beijing(Jing)-Tianjin(Jin)-Hebei(Ji) urban agglomeration. *Ecol. Indic.* **2022**, *137*, 108787. [[CrossRef](#)]
35. Chan, C.K.; Yao, X. Air pollution in mega cities in China. *Atmos. Environ.* **2008**, *42*, 1–42. [[CrossRef](#)]
36. Wu, X.; Ding, Y.; Zhou, S.; Tan, Y. Temporal characteristic and source analysis of PM2.5 in the most polluted city agglomeration of China. *Atmos. Pollut. Res.* **2018**, *9*, 1221–1230. [[CrossRef](#)]
37. Xia, X.; Chen, H.; Goloub, P.; Zong, X.; Zhang, W.; Wang, P. Climatological aspects of aerosol optical properties in North China Plain based on ground and satellite remote-sensing data. *J. Quant. Spectrosc. Radiat. Transf.* **2013**, *127*, 12–23. [[CrossRef](#)]
38. Song, Z.; Fu, D.; Zhang, X.; Wu, Y.; Xia, X.; He, J.; Han, X.; Zhang, R.; Che, H. Diurnal and seasonal variability of PM2.5 and AOD in North China plain: Comparison of MERRA-2 products and ground measurements. *Atmos. Environ.* **2018**, *191*, 70–78. [[CrossRef](#)]
39. Li, Z.; Chen, H.; Cribb, M.; Dickerson, R.; Holben, B.; Li, C.; Lu, D.; Luo, Y.; Maring, H.; Shi, G.; et al. Preface to special section on East Asian Studies of Tropospheric Aerosols: An International Regional Experiment (EAST-AIRE). *J. Geophys. Res.* **2007**, *112*, D22S00. [[CrossRef](#)]
40. Li, Z.; Li, C.; Chen, H.; Tsay, S.C.; Holben, B.; Huang, J.; Li, B.; Maring, H.; Qian, Y.; Shi, G.; et al. East Asian Studies of Tropospheric Aerosols and their Impact on Regional Climate (EAST-AIRC): An overview. *J. Geophys. Res.* **2011**, *116*, D00K34. [[CrossRef](#)]

41. Zhou, M.; Yang, Y.; Sun, Y.; Zhang, F.; Li, Y. Spatio-temporal Characteristics of Air Quality and Influencing Factors in Shandong Province from 2016 to 2020. *Environ. Sci.* **2022**, *43*, 2937–2946. [[CrossRef](#)]
42. Ministry of Ecology and Environmental of the People's Republic of China (MEEP). *China Environmental Status Bulletin 2019*; Ministry of Ecology and Environmental of the People's Republic of China: Beijing, China, 2020.
43. Sathe, Y.; Kulkarni, S.; Gupta, P.; Kaginalkar, A.; Islam, S.; Gargava, P. Application of Moderate Resolution Imaging Spectroradiometer (MODIS) Aerosol Optical Depth (AOD) and Weather Research Forecasting (WRF) model meteorological data for assessment of fine particulate matter (PM_{2.5}) over India. *Atmos. Pollut. Res.* **2019**, *10*, 418–434. [[CrossRef](#)]
44. Liu, N.; Zou, B.; Feng, H.; Wang, W.; Tang, Y.; Liang, Y. Evaluation and comparison of multiangle implementation of the atmospheric correction algorithm, Dark Target, and Deep Blue aerosol products over China. *Atmos. Chem. Phys.* **2019**, *19*, 8243–8268. [[CrossRef](#)]
45. Ghotbi, S.; Sotoudeheian, S.; Arhami, M. Estimating urban ground-level PM₁₀ using MODIS 3km AOD product and meteorological parameters from WRF model. *Atmos. Environ.* **2016**, *141*, 333–346. [[CrossRef](#)]
46. Wang, W.; Mao, F.; Pan, Z.; Du, L.; Gong, W. Validation of VIIRS AOD through a Comparison with a Sun Photometer and MODIS AODs over Wuhan. *Remote Sens.* **2017**, *9*, 403. [[CrossRef](#)]
47. You, Y.; Zhao, T.; Xie, Y.; Zheng, Y.; Zhu, J.; Xia, J.; Cao, L.; Wang, C.; Che, H.; Liao, Y.; et al. Variation of the aerosol optical properties and validation of MODIS AOD products over the eastern edge of the Tibetan Plateau based on ground-based remote sensing in 2017. *Atmos. Environ.* **2020**, *223*, 117257. [[CrossRef](#)]
48. Zhang, J.; Xin, J.; Zhang, W.; Wang, S.; Wang, L.; Xie, W.; Xiao, G.; Pan, H.; Kong, L. Validation of MODIS C6 AOD products retrieved by the Dark Target method in the Beijing–Tianjin–Hebei urban agglomeration, China. *Adv. Atmos. Sci.* **2017**, *34*, 993–1002. [[CrossRef](#)]
49. Shu, X.L.; Gao, Y.P.; Zhang, Y.X.; Yang, C.Y. Study on the Coupling Relationship and Coordinative Development between Tourism Industry and Ecocivilization City. *China Popul. Resour. Environ.* **2015**, *25*, 82–90. [[CrossRef](#)]
50. Cong, X.N. Expression and Mathematical Property of Coupling Model, and Its Misuse in Geographical Science. *Econ. Geogr.* **2019**, *39*, 18–25. [[CrossRef](#)]
51. Tian, S.; Yang, B.; Liu, Z.; Li, X.; Zhang, W. Coupling Coordination of Urban Pseudo and Reality Human Settlements. *Land* **2022**, *11*, 414. [[CrossRef](#)]
52. Hao, C.; Guo, L.; Wang, F.; Liu, M.; Jiao, L. Research on Coupling Degree of Atmospheric Aerosols and Pollutants in Beijing–Tianjin–Hebei Region. *J. North China Univ. Sci. Technol. Nat. Sci. Ed.* **2021**, *43*, 86–95.
53. Feng, D.; Shen, Q. Optimization of ecological environment in Shanghai based on correlation and coupling analysis. *Urban Plan. Forum* **2015**, *226*, 75–83. [[CrossRef](#)]
54. Ma, X.; Wang, J.; Yu, F.; Jia, H.; Hu, Y. Can MODIS AOD be employed to derive PM_{2.5} in Beijing–Tianjin–Hebei over China? *Atmos. Res.* **2016**, *181*, 250–256. [[CrossRef](#)]
55. Lin, G.; Fei, M.; Ming-liang, M. Spatiotemporal Variation and Influencing Factors of AOD in the North China Plain. *Environ. Sci.* **2022**, *43*, 3483–3493. [[CrossRef](#)]
56. Xue, R.; Ai, B.; Lin, Y.; Pang, B.; Shang, H. Spatial and Temporal Distribution of Aerosol Optical Depth and Its Relationship with Urbanization in Shandong Province. *Atmosphere* **2019**, *10*, 110. [[CrossRef](#)]
57. Zhou, Z.; Wang, Z.; Shi, J.; Zhong, Y.; Ding, Y. Variation Characteristics and Source Analysis of Pollutants in Jinghong before and after the COVID-19 Pandemic. *Atmosphere* **2022**, *13*, 1846. [[CrossRef](#)]
58. Dang, H.-A.H.; Trinh, T.-A. Does the COVID-19 lockdown improve global air quality? New cross-national evidence on its unintended consequences. *J. Environ. Econ. Manag.* **2021**, *105*, 102401. [[CrossRef](#)] [[PubMed](#)]
59. Zheng, Y.; Wang, X.; Zhang, X.; Hu, G. Multi-spatiotemporal patterns of aerosol optical depth and influencing factors during 2000–2020 from two spatial perspectives: The entire Yellow River Basin region and its urban agglomerations. *Int. J. Appl. Earth Obs. Geoinf.* **2022**, *106*, 102643. [[CrossRef](#)]
60. Deng, B.; Li, C.K.; Ji, Y.L. Analysis on the Treatment of Volatile Organic Compounds (VOCs) in Dongying City. *China Stand.* **2021**, *581*, 87–93. [[CrossRef](#)]
61. Wu, H.; Gao, X.; Ma, Z.; Zhang, S. Effectiveness of production reduction policy on improving air quality in Dongying. *IOP Conf. Ser. Earth Environ. Sci.* **2019**, *227*, 052043. [[CrossRef](#)]
62. Jiang, S.; Yu, H.; Li, Z.; Geng, B.; Li, T. Study on the Evolution of the Spatial-Temporal Pattern and the Influencing Mechanism of the Green Development Level of the Shandong Peninsula Urban Agglomeration. *Sustainability* **2022**, *14*, 9549. [[CrossRef](#)]
63. Meng, Q.; Bai, H.Y.; Zhao, T.; Guo, S.Z.; Qi, G.Z. The eco-barrier effect of Qinling Mountain on aerosols. *Remote Sens. Land Resour.* **2021**, *33*, 240–248. [[CrossRef](#)]
64. Rodríguez, S.; Cuevas, E.; González, Y.; Ramos, R.; Romero, P.M.; Pérez, N.; Querol, X.; Alastuey, A. Influence of sea breeze circulation and road traffic emissions on the relationship between particle number, black carbon, PM₁, PM_{2.5} and PM_{2.5–10} concentrations in a coastal city. *Atmos. Environ.* **2008**, *42*, 6523–6534. [[CrossRef](#)]
65. Yli-Juuti, T.; Mielonen, T.; Heikkinen, L.; Arola, A.; Ehn, M.; Isokääntä, S.; Keskinen, H.-M.; Kulmala, M.; Laakso, A.; Lipponen, A.; et al. Significance of the organic aerosol driven climate feedback in the boreal area. *Nat. Commun.* **2021**, *12*, 5637. [[CrossRef](#)] [[PubMed](#)]

66. Shi, D.; Liu, J.; Wang, Y.; Xu, L.; Guo, T.; Jia, B.; Cheng, P. Secondary organic aerosol formation from cis-3-hexen-1-ol/NO_x photo-oxidation: The roles of cis-3-hexen-1-ol concentration, illumination intensity, NO_x and NH₃. *Atmos. Environ.* **2022**, *278*, 119090. [[CrossRef](#)]
67. Nam, J.; Kim, S.-W.; Park, R.J.; Park, J.-S.; Park, S.S. Changes in column aerosol optical depth and ground-level particulate matter concentration over East Asia. *Air Qual. Atmos. Health* **2018**, *11*, 49–60. [[CrossRef](#)]
68. Zhang, C. AQI Characteristics and Meteorological Cause Analysis of Severe Air Pollution Process in Heze City in Early May 2017. *Sichuan Environ.* **2020**, *39*, 51–56. [[CrossRef](#)]
69. Cheng, Y.; Liu, B.; Wu, J.; Zhang, Q.; Feng, Y.; Bi, X.; Zhang, Y. Pollution characteristics of water-soluble ions in ambient PM₁₀ and PM_{2.5} during summer of 2015 in Heze City. *Environ. Chem.* **2019**, *38*, 729–737. [[CrossRef](#)]
70. Zhu, Z.; Qiao, Y.; Liu, Q.; Lin, C.; Dang, E.; Fu, W.; Wang, G.; Dong, J. The impact of meteorological conditions on Air Quality Index under different urbanization gradients: A case from Taipei. *Environ. Dev. Sustain.* **2021**, *23*, 3994–4010. [[CrossRef](#)]
71. Di, Y.; Li, R. Correlation analysis of AQI characteristics and meteorological conditions in heating season. *IOP Conf. Ser. Earth Environ. Sci.* **2019**, *242*, 022067. [[CrossRef](#)]
72. He, L.; Wang, L.; Huang, B.; Wei, J.; Zhou, Z.; Zhong, Y. Anthropogenic and meteorological drivers of 1980–2016 trend in aerosol optical and radiative properties over the Yangtze River Basin. *Atmos. Environ.* **2020**, *223*, 117188. [[CrossRef](#)]
73. Augustin, P.; Billet, S.; Crumeyrolle, S.; Deboudt, K.; Dieudonné, E.; Flament, P.; Fourmentin, M.; Guilbaud, S.; Hanoune, B.; Landkocz, Y.; et al. Impact of Sea Breeze Dynamics on Atmospheric Pollutants and Their Toxicity in Industrial and Urban Coastal Environments. *Remote Sens.* **2020**, *12*, 648. [[CrossRef](#)]
74. VishnuRadhan, R.; Thresyamma, D.D.; Eldho, T.I.; Dhiman, R.; Bhavan, S.G. On the emergence of a health-pollutant-climate nexus in the wake of a global pandemic. *Environ. Sci. Pollut. Res.* **2022**, *29*, 85619–85631. [[CrossRef](#)]
75. Sahraei, M.A.; Kuşkan, E.; Çodur, M.Y. Public transit usage and air quality index during the COVID-19 lockdown. *J. Environ. Manag.* **2021**, *286*, 112166. [[CrossRef](#)]
76. Xu, T.; Yan, H.; Bai, Y. Air Pollutant Analysis and AQI Prediction Based on GRA and Improved SOA-SVR by Considering COVID-19. *Atmosphere* **2021**, *12*, 336. [[CrossRef](#)]
77. Li, W.; Shao, L.; Zhang, D.; Ro, C.-U.; Hu, M.; Bi, X.; Geng, H.; Matsuki, A.; Niu, H.; Chen, J. A review of single aerosol particle studies in the atmosphere of East Asia: Morphology, mixing state, source, and heterogeneous reactions. *J. Clean. Prod.* **2016**, *112*, 1330–1349. [[CrossRef](#)]
78. Li, Q.; Ji, M.; Sun, Y.; Zhai, X.; Zheng, Y. Analysis and evaluation of air quality in Shandong province based on AHP. *IOP Conf. Ser. Earth Environ. Sci.* **2021**, *651*, 042033. [[CrossRef](#)]
79. Jin, X.; Cai, X.; Yu, M.; Song, Y.; Wang, X.; Kang, L.; Zhang, H. Diagnostic analysis of wintertime PM_{2.5} pollution in the North China Plain: The impacts of regional transport and atmospheric boundary layer variation. *Atmos. Environ.* **2020**, *224*, 117346. [[CrossRef](#)]
80. Wang, Z.; Yan, J.; Zhang, P.; Li, Z.; Guo, C.; Wu, K.; Li, X.; Zhu, X.; Sun, Z.; Wei, Y. Chemical characterization, source apportionment, and health risk assessment of PM_{2.5} in a typical industrial region in North China. *Environ. Sci. Pollut. Res.* **2022**, *29*, 71696–71708. [[CrossRef](#)]
81. Gharibzadeh, M.; Bidokhti, A.A.; Alam, K. The interaction of ozone and aerosol in a semi-arid region in the Middle East: Ozone formation and radiative forcing implications. *Atmos. Environ.* **2021**, *245*, 118015. [[CrossRef](#)]
82. Chawala, P.; Priyan, R.S.; Sm, S.N. Climatology and landscape determinants of AOD, SO₂ and NO₂ over Indo-Gangetic Plain. *Environ. Res.* **2023**, *220*, 115125. [[CrossRef](#)]
83. Xu, J.; Jia, H.; Zhou, H.; Kang, Y.; Zhong, K. Influences of offshore background wind on the formation of sea-land breeze and the characteristics of pollutant diffusion. *Environ. Sci. Pollut. Res.* **2021**, *28*, 68318–68329. [[CrossRef](#)]
84. Zhang, X.; Gu, X.; Cheng, C.; Yang, D. Spatiotemporal heterogeneity of PM_{2.5} and its relationship with urbanization in North China from 2000 to 2017. *Sci. Total Environ.* **2020**, *744*, 140925. [[CrossRef](#)]
85. Liu, X.; Wang, Y.; Liu, R.; Zhang, Y.; Shao, L.; Han, K.; Zhang, Y. 2328 Pollution characteristics, source identification and potential ecological risk of 50 elements in atmospheric particulate matter during winter in Qingdao. *Arab. J. Geosci.* **2022**, *15*, 233. [[CrossRef](#)]
86. Xing, H.; Zhu, L.; Chen, B.; Niu, J.; Li, X.; Feng, Y.; Fang, W. Spatial and temporal changes analysis of air quality before and after the COVID-19 in Shandong Province, China. *Earth Sci. Inform.* **2022**, *15*, 863–876. [[CrossRef](#)]
87. Ju, T.; Pan, B.; Li, B.; Wang, J.; Liu, S.; Peng, S.; Li, M. A Characteristic Analysis of Various Air Pollutants and Their Correlation with O₃ in the Jiangsu, Shandong, Henan, and Anhui Provinces of China. *Sustainability* **2022**, *14*, 13737. [[CrossRef](#)]
88. Cichowicz, R.; Wielgosiński, G.; Fetter, W. Dispersion of atmospheric air pollution in summer and winter season. *Environ. Monit. Assess.* **2017**, *189*, 605. [[CrossRef](#)] [[PubMed](#)]
89. Li, Y.; Miao, Y.; Che, H.; Liu, S. On the heavy aerosol pollution and its meteorological dependence in Shandong province, China. *Atmos. Res.* **2021**, *256*, 105572. [[CrossRef](#)]

Disclaimer/Publisher's Note: The statements, opinions and data contained in all publications are solely those of the individual author(s) and contributor(s) and not of MDPI and/or the editor(s). MDPI and/or the editor(s) disclaim responsibility for any injury to people or property resulting from any ideas, methods, instructions or products referred to in the content.